Original Article

Identification of Q-Markers from Hedan Tablet by employing "spider-web" mode and taking compounds' hepatotoxicity into account

Danni Wang [a,1], Jiamin Ding [a,1], Xiafei Feng [b], Xin Chai [a], Jing Yang [a], Chunlei Liu [c], Yingzi Zeng [c], Wanhui Zhou [c,*], Yuefei Wang [a,*]

[a] State Key Laboratory of Component-based Chinese Medicine, Tianjin Key Laboratory of TCM Chemistry and Analysis, Tianjin University of Traditional Chinese Medicine, Tianjin 301617, China
[b] Foreign Language College, Donghua University, Shanghai 201620, China
[c] Shandong Wohua Pharmaceutical Technology Co., Ltd., Weifang 261000, China

ARTICLE INFO

ABSTRACT

Objective: Due to the complicated compounds and the synergistic effect of multi-compounds, the quality control and assessment of Chinese materia medica (CMM) encounters a great challenge about how to identify the key compounds, which are directly correlated with its efficacy and safety. On the guidance of study on quality marker (Q-Marker), identification of Q-Markers was performed from Hedan Tablet (HDT) by the aid of the "spider-web" mode and hepatotoxicity evaluation derived from our previous researches and literatures.
Methods: By the established ultra performance liquid chromatography with photodiode array detector (UPLC-PDA) method, online UPLC-DPPH· and offline antioxidant assay, 21 candidate compounds of HDT were systematically investigated and comprehensively evaluated by the "spider-web" mode for them properties of Q-Marker based on "content-stability-activity". In addition, the Q-Markers related with hepatotoxicity based on our previous researches and literatures were identified.
Results: Salvianolic acid B (SaB), quercetin-3-O-glucuronide (Qug), isoquercitrin (IQ) and hyperoside (Hyp) were adopted as the preferable Q-Markers of HDT according to the shaded area (A) of tested compounds in "spider-web" mode. Psoralen (Ps), isopsoralen (IP), psoralenoside (PO) and isopsoralenoside (IPO) were also strongly recommended as Q-Markers closely related with safety by considering hepatotoxicity of the accumulated Ps and IP and conversion between glycoside (PO and IPO) and aglycone (Ps and IP).
Conclusion: This study provided scientific evidence for quality control and assessment of HDT, and also provided a meaningful reference for application of Q-Markers in CMM.

1. Introduction

Hyperlipidemia, characterized by dyslipidemia, is one of the main hazard factors for development and progression of metabolic disease and cardiovascular disease, leading to high morbidity in modern society (Navar-Boggan et al., 2015; Pencina et al., 2014). Although many lipid-lowering drugs including statins, ezetimibe and fibrates have been developed (Davidson & Toth, 2004), hyperlipidemia treatment still has many difficulties due to the fact that these drugs can not address all facets of dyslipidemia and the increased risk derived from many adverse reactions (Hajdu et al., 2009; Ho et al., 2004; Wierzbicki et al., 2012). As a complementary and alternative medicine to western medicine, Chinese materia medica (CMM) provides an integrated and unique approach to treat hyperlipidemia (Sham et al., 2014). Moreover, herbal therapy may provide a more sustainable treatment due to its low incidence of side effects (Li et al., 2020b). In recent years, lots of Chinese herbal medicines and its preparations have been demonstrated to have potent hypolipidemic effect, such as *Salviae Miltiorrhizae Radix* et *Rhizoma*, *Notoginseng Radix* et *Rhizoma*, Xuefu Zhuyu Decoction, Xuezhikang Capsule, and so on (Li et al., 2020b; Liao et al., 2014; Xia et al., 2011; Zhao et al., 2003). They exert hypolipidemic effect through a variety of mechanisms, such as decreasing

* Corresponding authors.
  E-mail addresses: zhou_wanhui@163.com (W. Zhou), wangyf0622@tjutcm.edu.cn (Y. Wang).
  [1] These authors contributed equally to this work.

cholesterol absorption and synthesis, regulating cholesterol transport and transcription factors related to lipid metabolism, and promoting cholesterol excretion (Li et al., 2013; Li et al., 2017). In addition, studies have shown that antioxidant activity including alleviation of oxidative stress and lipid peroxidation, and increase of antioxidant enzyme could strengthen its anti-hyperlipidemia (Hong et al., 2006; Wu et al., 1998; Xia et al., 2011). Therefore, our study preliminarily evaluated the tested compounds in Hedan Tablet (HDT) from the perspective of antioxidant activity.

As a Chinese patent medicine, HDT, composed of *Nelumbinis Folium* (Heye in Chinese, as monarch drug), *Salviae Miltiorrhizae Radix* et *Rhizoma* (Danshen in Chinese, as minister drug), *Psoraleae Fructus* (Buguzhi in Chinese as minister drug), *Crataegi Fructus* (Shanzha in Chinese, as assistant drug), and *Sennae Folium* (Fanxieye in Chinese, as guide drug), is the effective drug with functions of removing phlegm and turbidity, activating blood circulation, and removing blood stasis (Chen et al., 2011; Sun et al., 2017). Clinical studies have demonstrated that HDT has a remarkable curative effect on hyperlipidemia (Li, 2012; Xu et al., 2016; Zhang et al., 2015). Also, it can be combined with western medicines (statins and metformin) for treating acute cerebral infarction, coronary heart disease, diabetes, nonalcoholic fatty liver disease, and so on (Cai, 2018; Li et al., 2016; Tian, 2010; Wang, 2015). At present, in *Chinese Pharmacopoeia*, only nuciferine (Nuc) is adopted as the marker compound for quality control and assessment of HDT (Chinese Pharmacopoeia Commission, 2020). And few researchers established LC methods for the simultaneous determination of multi-compounds in HDT (Liu et al., 2011; Zhao and Tang, 2013). However, the effect of HDT cannot be reflected by only a few chemical ingredients, and there is a lack of sufficient evidence to support that the determined compounds can be chosen as the quality markers (Q-Markers). In recent years, the China National Center for ADR Monitoring has frequently reported that the clinical application of *Psoraleae Fructus*-related preparations caused severe liver injury. Therefore, the control of hepatotoxic compounds derived from *Psoraleae Fructus* in HDT is also particularly paramount due to liver injury of *Psoraleae Fructus* (Cheung et al., 2009; Tian et al., 2017). Fortunately, under the guidance of the Q-Marker theory proposed by Academician Changxiao Liu, it sheds the light for the quality control of CMM related preparations with the complicated compounds (Liu et al., 2016; Liu et al., 2017; Liu, 2021). In order to identify Q-Markers from CMM related preparations, "spider-web" mode was successfully developed and extended to apply in stability study, optimization of extracting methods and processing parameters, screening of active fractions, and so on (Li et al., 2019b; Wang et al., 2016; Yang et al., 2018; Yu et al., 2018; Zhang et al., 2019a). "Spider-web" mode based on "content-stability-activity" has been proven to be a great strategy, which can filter out the redundant compounds and focus on the key indexes of quality control (Zhang et al., 2020).

In our study, with the help of the "spider-web" mode and hepatotoxicity evaluation derived from our previous researches and literatures, identification of Q-Markers was performed from HDT by taking effectiveness and safety into account. Based on the comprehensive analysis of the main compounds of each CMM and the quality control indicators of HDT in the *Chinese Pharmacopoeia*, 21 compounds were finally selected as candidate compounds, including astragaline (Ast), bakuchiol (Bak), corylin (Cor), cryptotanshinone (Cry), hyperoside (Hyp), isopsoralen (IP), isopsoralenoside (IPO), isoquercitrin (IQ), lithospermic acid (Lia), neobavaisoflavone (Neo), Nuc, psoralen (Ps), psoralenoside (PO), quercetin-3-O-glucuronide (Qug), rhein (Rhe), rosmarinic acid (Roa), salvianolic acid A (SaA), salvianolic acid B (SaB), salvianolic acid C (SaC), sennoside A (SeA) and sennoside B (SeB). The UPLC-PDA method was constructed and employed to analyze the content and stability of candidate compounds in HDTs. Online UPLC-DPPH· method com-

bined offline antioxidant assay was used to screen compounds with antioxidant activity from HDT. The content, stability and activity of compounds, the important elements affecting effectiveness of HDT, were used as three dimensions to construct "spider-web" mode. And the effectiveness-related Q-Markers were selected based on the analytic result by the "spider-web" mode. In addition, the Q-Markers related with hepatotoxicity were identified based on our previous researches and literatures.

2. Materials and methods

2.1. Reagents and materials

HPLC-grade methanol and acetonitrile, and analytical grade DPPH· were purchased from Sigma-Aldrich Inc. (St. Louis, MO, USA). HPLC-grade formic acid was obtained from Shanghai Aladdin Biochemical Technology Co. Ltd. (Shanghai, China). Water employed in the experiment was purified by a Milli-Q water purification system (Millipore, Billerica, USA). Ten batches of HDTs, numbered as B1–B10, were provided by Nanchang Jishun Pharmaceutical Co., Ltd. (Nanchang, China). Cry, Hyp and Nuc were purchased from Shanghai Yuanye Bio-Technology Co., Ltd. (Shanghai, China). Qug, IQ, SeA, SeB and Lia were purchased from Chengdu Herbpurify Co., Ltd. (Chengdu, China). Roa, SaA, SaB and SaC were obtained from Zhongxin Innova Laboratories (Tianjin, China). Ast was purchased from Hebei Tuohai Biotechnology Co., Ltd. (Handan, China). Rhe was purchased from the National Institute for Food and Drug Control (Beijing, China). Ps, IP, PO, IPO, Neo, Cor and Bak were prepared in our laboratory. The purity of all reference compounds was above 98% by LC-UV analysis.

2.2. Preparation of reference and sample solutions

Reference compounds were accurately weighed and dissolved with a little of DMSO and methanol to obtain respective stock solution at the concentration of 2 mg/mL for PO, IPO, Hyp, Qug, IQ and IP and 1 mg/mL for SeB, Ast, SeA, Roa, Lia, SaB, Nuc, SaA, Ps, SaC, Rhe, Neo, Cor, Cry and Bak. Then, the mixed stock standard solution was prepared by employing stock standard solution of 21 compounds to reach the final concentration at PO 137.0 μg/mL, IPO 78.23 μg/mL, Hyp 133.6 μg/mL, Qug 165.4 μg/mL, IQ 75.59 μg/mL, SeB 6.370 μg/mL, Ast 24.78 μg/mL, SeA 8.212 μg/mL, Roa 16.04 μg/mL, Lia 16.73 μg/mL, SaB 211.5 μg/mL, Nuc 53.81 μg/mL, SaA 35.04 μg/mL, Ps 21.42 μg/mL, IP 31.64 μg/mL, SaC 5.907 μg/mL, Rhe 22.48 μg/mL, Neo 4.030 μg/mL, Cor 0.8905 μg/mL, Cry 13.29 μg/mL and Bak 9.904 μg/mL. Subsequently, the working solutions at the different concentrations were diluted for constructing calibration curves. All standard solutions were stored at 4 °C for further analysis.

The accurately weighed sample powder (0.5 g) was transferred into 25 mL volumetric flask and ultrasonically extracted by methanol for 15 min, then cooled to ambient temperature and diluted to scale by adding methanol. The extracted solution was centrifuged at 14 000 rpm for 10 min to obtain the supernatant and diluted with 50% methanol (volume percentage, 1:1) to obtain the sample solution.

2.3. UPLC-PDA conditions

Equipped with a quaternary solvent delivery pump, an autosampler and PDA detector, ACQUITY UPLC H-class system (Waters Corporation, Milford, MA, USA) was used to perform the chromatographic analysis by using ACQUITY UPLC® BEH C$_{18}$ column (100 mm × 2.1 mm, 1.7 μm) at 40 °C. The mobile phase was composed of 0.1% formic acid aqueous solution (A) and ace-

tonitrile (B) and implemented in the gradient elution at a flow rate of 0.3 mL/min as follows: 3%–11% B in 0–5 min, 11%–13% B in 5–9 min, 13%–15% B in 9–12 min, 15%–23% in 12–14.1 min, 23%–26.5% B in 14.1–19 min, 26.5%–90% B in 19–28 min, 90% B in 28–30 min. The tested solution (2 μL) was injected for analysis. The following switching program of multi-wavelength was employed: 0–8 min, 254 nm; 8–10.5 min, 246 nm; 10.5–13.2 min, 254 nm; 13.2–14.85 min, 264 nm; 14.85–15.8 min, 331 nm; 15.8–16.7 min, 309 nm; 16.7–17.2 min, 270 nm; 17.2–17.8 min, 254 nm; 17.8–19.5 min, 246 nm; and 19.5–30 min, 254 nm.

2.4. Quantitative method validation

The analytic method established in this study was implemented to validate linearity, limit of detection (LOD), limit of quantitation (LOQ), precision (intra- and inter-day), stability and recovery. The calibration curves were constructed in duplicate using the peak area (y axis) and the corresponding concentration of standard solution (x axis). The LOQ and LOD for the tested compounds were determined by gradually decreasing concentration of the standard solution until signal was 10 and 3 at signal-to-noise ratio (S/N), respectively. The sample solution was repeatedly injected at six times on the same day and three consecutive days to test the intra- and inter-day precision, respectively. Repeatability was confirmed by preparing and analysing six sample solutions in parallel. The stability was studied by injecting sample solution at 0, 2, 4, 6, 8, 10 and 12 h, respectively. The recovery test was conducted by adding standard solution to 0.25 g sample powder (n = 6), which was processed according to the method of sample preparation.

2.5. Stability study of HDTs

The HDTs were stored in the stability test chamber (ClimaceII 222, MMM group, Germany) under high temperature [60 °C, RH (40 ± 5)%], high humidity [(25 °C, RH (90 ± 5)%] and strong light [4500 Lx ± 500 Lx, 25 °C, RH (40 ± 5)%] for 10 d, respectively. The samples were collected at 0, 5 and 10 d and measured in duplicate by the established UPLC-PDA method.

2.6. Antioxidant assay

Online UPLC-DPPH· Assay: The accurately weighed HDT powder (2.0 g) was transferred into 50 mL volumetric flask and ultrasonically extracted by methanol for 20 min, then cooled to room temperature and diluted to the scale by methanol. The extracted solution was centrifuged at 14 000 rpm for 10 min to obtain the sample solution at 40 mg/mL (HDT extract). HDT extract (5 mL) was precisely transferred to 10 mL volumetric flask, added by 1200 μL DPPH· methanolic solution (5 mg/mL) and diluted to scale by adding 50% methanol, then shaken with the constant temperature culture oscillator (HNY-200B, Honour Instrument Shaker, Tianjin, China) for 15 min (37 °C) in the dark. After that, the reacted sample solution was centrifuged at 14 000 rpm for 10 min, and the supernatant (2 μL) was injected into UPLC for analysis by the established UPLC-PDA method. The sample solution was mixed with methanol to obtain the control solution according to the procedure for preparing the reacted sample solution.

Offline Antioxidant Assay: The DPPH· microporous quantitative assay was applied to detect the antioxidant activity of HDT and 18 candidate compounds except for the undetected compounds (SeA, SeB and SaC). Reference standards were accurately weighed and dissolved with a little of DMSO and methanol to obtain respective stock solution as follows: IQ, 0.522 mg/mL; Roa, 0.970 mg/mL; Ast, 2.882 mg/mL; Lia, 0.355 mg/mL; SaB, 0.252 mg/mL; Qug, 0.486 mg/mL; Hyp, 0.489 mg/mL; SaA, 0.480 mg/mL; Rhe, 2.484 mg/mL; PO, 2.360 mg/mL; IPO, 2.834 mg/mL; Ps,

2.912 mg/mL; IP, 2.860 mg/mL; Neo, 3.024 mg/mL; Nuc, 3.120 mg/mL; Cor, 3.100 mg/mL; Cry, 0.494 mg/mL; Bak, 1.338 mg/mL. Then, the HDT sample solution (20 mg/mL) and the stock standard solutions were diluted with methanol to prepare a series of the tested sample solutions. The tested sample solution (50 μL) was mixed with 150 μL of DPPH· methanolic solution (0.1 mg/mL) in a 96-well microplate (Corning Incorporated, Corning, NY, USA). The blank solution was prepared by mixing the tested sample solution (50 μL) with methanol (150 μL), while methanol (50 μL) was added to DPPH· methanolic solution (150 μL) as the control solution. The prepared solution was incubated for 45 min at 37 °C in the darkroom, the value of optical density (OD) of which was measured at 512 nm with a microplate reader (Tecan Spark 10M, Switzerland). All tests were operated three times in parallel. The DPPH· scavenging rate was measured using the following Eq. (1):

$$SR(\%) = [1 - (OD_{sample} - OD_{blank})/OD_{control}] \times 100\% \tag{1}$$

where OD_{sample}, OD_{blank} and $OD_{control}$ are the OD values of the sample, blank and control solution, respectively. The antioxidant activity was expressed by the half maximal inhibitory concentration (IC$_{50}$) value calculated from the dose–effect curve.

2.7. Data analysis

The data was subjected to statistical analysis by Excel 2016.Lnk software. Dose-effect curve fitted by nonlinear curve analysis, "spider-web" mode, 3D bar graph, box diagram, double-Y charts and bar charts were plotted using Origin 9.1 software (OriginLab, Northampton, MA, USA).

3. Results and discussion

3.1. Methodological validation of UPLC-PDA analysis for quantitation of 21 candidate compounds

Aiming at the excellent separation and sensitivity of the tested compounds, the program of gradient elution, column temperature and the switching program of multi-wavelength were systematically optimized. Also, the method for sample preparation was determined in the light of the systematical study on influencing factor, such as extracted solvent, time and material-liquid ratio. Upon the optimized condition, the typical chromatograms of sample and mixed standard solution were presented in Fig. 1.

As shown in Table 1, the simultaneous quantification of multi-compounds in HDT was validated. The calibration curves of 21 tested compounds were established with the determination coefficient (r^2) exceeding 0.9944, which indicated a good linear correlation within the test ranges. The LOD and LOQ were 0.0033–0.1226 μg/mL and 0.0100–0.3678 μg/mL, respectively. For quantified compounds, the RSDs of the intra-day and inter-day precisions were 0.6%–2.1% and 0.6%–1.9%, respectively. The RSD of repeatability was proven below 3.3%. The result of stability test, with RSD less than 2.7%, showed that the determined compounds in sample solution were stable within 12 h. The mean recovery was in the range of 91.36%–111.6% with RSD less than 3.5%. All results demonstrated that the established method was stable and reliable for the simultaneous determination of 21 candidate compounds in HDT.

3.2. Establishment of content dimension of "spider-web" mode upon quantified result of 21 candidate compounds in HDTs

Ten batches of HDTs manufactured between 2017 and 2018 by the manufacturer were subjected to UPLC analysis to determine
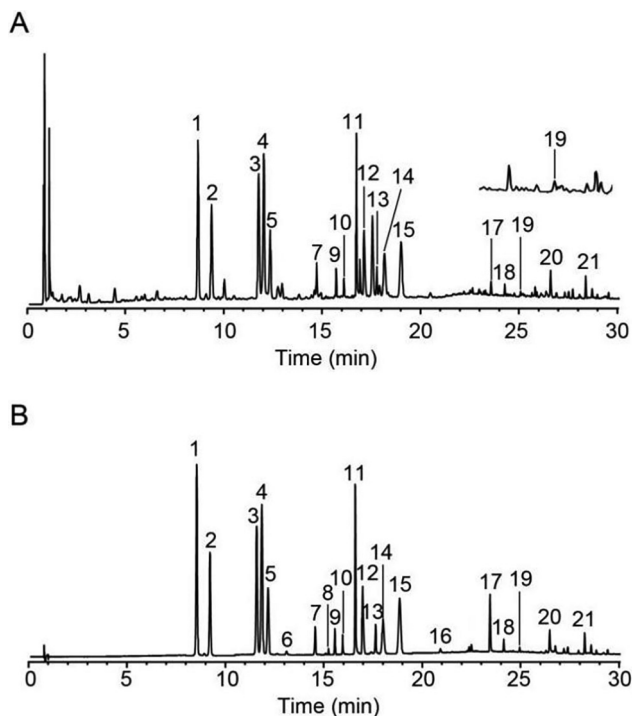
Fig. 1. UPL of HDT sample solution (A) and mixed standard solution (B). (1, psoralenoside; 2, isopsoralenoside; 3, hyperoside; 4, quercetin-3-O-glucuronide; 5, isoquercitrin; 6, sennoside B; 7, astragaline; 8, sennoside A; 9, rosmarinic acid; 10, lithospermic acid; 11, salvianolic acid B; 12, nuciferine; 13, salvianolic acid A; 14. psoralen; 15, isopsoralen; 16, salvianolic acid C; 17, rhein; 18, neobavaisoflavone; 19, corylin; 20, cryptotanshinone; 21, bakuchiol).

the content of 21 candidate compounds by the developed method. The quantified results of 21 candidate compounds in 10 batches of HDTs were shown in Table S1. As displayed in Fig. 2A and B, SaB (3. 556–4.516 mg/g), Qug (3.096–4.303 mg/g), Hyp (2.322–3.636 mg/

g), PO (2.164–2.474 mg/g), IQ (1.575–2.300 mg/g), IPO (1.683–1.923 mg/g) and Nuc (1.113–1.637 mg/g) were exceedingly abundant compounds in the tested HDT samples, accounting for 85% of the total content of 21 candidate compounds. Moreover, Ast (0.5 256–0.7859 mg/g), Ps (0.4227–0.5382 mg/g), IP (0.2576–0.4459 m g/g), Lia (0.3194–0.3924 mg/g), Cry (0.2081–0.3533 mg/g), Roa (0. 2524–0.2939 mg/g), SaA (0.1335–0.5988 mg/g) and Bak (0.1388–0. 2203 mg/g), between 0.1 and 1.0 mg/g, were deemed to be the second level. Rhe (0.07731–0.1109 mg/g), Neo (0.06793–0.1066 mg/g) and Cor (0.01012–0.03503 mg/g) were assigned to the third level with content ranging from 0.01 to 0.1 mg/g in almost all HDT samples. SeA, SeB and SaC were not detected in 10 batches of HDTs, which may be caused by degradation during preparation (Goppel & Franz, 2004; Liu et al., 2015). Undoubtedly, the above result confirmed that there is a remarkable difference in the content of the tested compounds of HDTs. And, an obvious fluctuation of content was found among the interesting compounds from different batches samples, indicating that it is urgent for us to establish a scientific and reasonable method for quality control of HDT. Therefore, the identification of Q-Markers is imperative. Focusing on solving this problem, we employed the "spider-web" mode to perform systematical study based on "content-stability-activity".

In order to successfully construct content dimension of "spider-web" mode and decrease the analytical deviation caused by large divergence on content of the quantified compounds, it is indispensable to normalize the quantitative result of tested compounds according to the following Eq. (2). The normalized result (content dimension value, CD) in the range of 0 and 1 can be employed to establish the content dimension of "spider-web" mode for identification of Q-Markers in HDT.

$$CD_n = \bar{C}_n / \bar{C}_{max} \tag{2}$$

where CD_n is the normalized value for constructing the content dimension of the tested compound n; $\bar{C}_n$ is the mean content of the tested compound n in 10 batches of HDTs; $\bar{C}_{max}$ is the maximum value of mean content among the 21 tested compounds.

Table 1
Methodological validation for simultaneous quantification of 21 candidate compounds in HDT.

| Compounds	Linear regression			LOD	LOQ	Precision (RSD, %)		Repeatability	Stability	Recovery
	Regression equation	r^2	Linear range (μg/mL)	(μg/mL)	(μg/mL)	Intra-day	Inter-day	(n = 6, RSD, %)	(n = 7, RSD, %)	(n = 6, Mean ± SD, %)
Psoralenoside	$y = 20071\,x - 3006.9$	>0.9999	2.140–137.0	0.0793	0.2378	0.8	1.4	0.8	0.4	107.7 ± 1.2
Isopsoralenoside	$y = 19967\,x - 2041.1$	>0.9999	1.222–78.23	0.0452	0.1356	0.9	1.9	0.9	0.6	99.64 ± 1.0
Hyperoside	$y = 15752\,x - 3165.5$	>0.9999	2.087–133.6	0.0774	0.2322	1.1	0.7	1.0	1.6	108.3 ± 0.9
Quercetin-3-O-glucuronide	$y = 15378\,x - 8298.4$	>0.9999	2.584–165.4	0.0956	0.2867	1.1	0.6	2.1	0.5	106.7 ± 0.4
Isoquercitrin	$y = 14789\,x - 1819.8$	>0.9999	1.181–75.59	0.0437	0.1311	0.9	0.9	1.3	0.8	100.3 ± 1.2
Sennoside B	$y = 7530\,x - 242.19$	0.9999	0.09956–6.372	0.0333	0.0996	–	–	–	–	101.4 ± 3.5
Astragaline	$y = 13890\,x - 502.64$	>0.9999	0.3871–24.78	0.0433	0.1300	1.1	1.0	1.1	2.7	111.6 ± 0.9
Sennoside A	$y = 4898.5\,x - 65.489$	0.9999	0.1283–8.212	0.0433	0.1283	–	–	–	–	101.6 ± 2.8
Rosmarinic acid	$y = 14923\,x - 1344.0$	0.9998	0.2507–16.04	0.0278	0.0833	0.7	1.4	1.6	1.8	111.6 ± 0.7
Lithospermic acid	$y = 9766.2\,x - 92.170$	>0.9999	0.2614–16.73	0.0289	0.0867	1.1	1.6	2.0	0.7	98.42 ± 1.7
Salvianolic acid B	$y = 7284.2\,x - 5933.7$	0.9998	3.3051–211.5	0.1226	0.3678	0.6	0.8	0.2	0.5	102.3 ± 0.7
Nuciferine	$y = 19657\,x - 755.35$	>0.9999	0.8408–53.81	0.0933	0.2800	1.0	0.6	1.3	1.0	103.4 ± 0.4
Salvianolic acid A	$y = 8586.6\,x - 2426.9$	0.9998	0.5475–35.04	0.0611	0.1833	0.8	0.7	2.0	0.6	102.0 ± 1.4
Psoralen	$y = 38654\,x - 2196.7$	>0.9999	0.3346–21.42	0.0367	0.1100	1.1	1.0	1.0	0.7	100.2 ± 1.6
Isopsoralen	$y = 44796\,x - 3623.0$	>0.9999	0.4944–31.64	0.0544	0.1633	0.9	0.9	1.0	0.5	97.95 ± 1.3
Salvianolic acid C	$y = 9395.7\,x - 384.83$	0.9998	0.09230–5.907	0.0300	0.0923	–	–	–	–	99.50 ± 1.1
Rhein	$y = 25164\,x - 2830.83$	0.9999	0.3513–22.48	0.0389	0.1167	0.7	1.0	1.1	1.1	105.1 ± 3.2
Neobavaisoflavone	$y = 22412\,x + 107.95$	>0.9999	0.0630–4.030	0.0200	0.0600	0.9	0.8	1.1	1.2	100.1 ± 1.7
Corylin	$y = 40616\,x - 121.02$	0.9998	0.01391–0.8905	0.0033	0.0100	2.1	1.5	1.2	1.0	93.56 ± 2.6
Cryptotanshinone	$y = 8716\,x - 9390.9$	0.9944	0.2077–13.29	0.0700	0.2100	0.9	0.9	2.6	0.8	110.2 ± 1.8
Bakuchiol	$y = 17552\,x - 520.73$	>0.9999	0.1548–9.904	0.0500	0.1500	0.9	0.9	3.3	0.7	91.36 ± 1.1

"–", Signal below LOD.
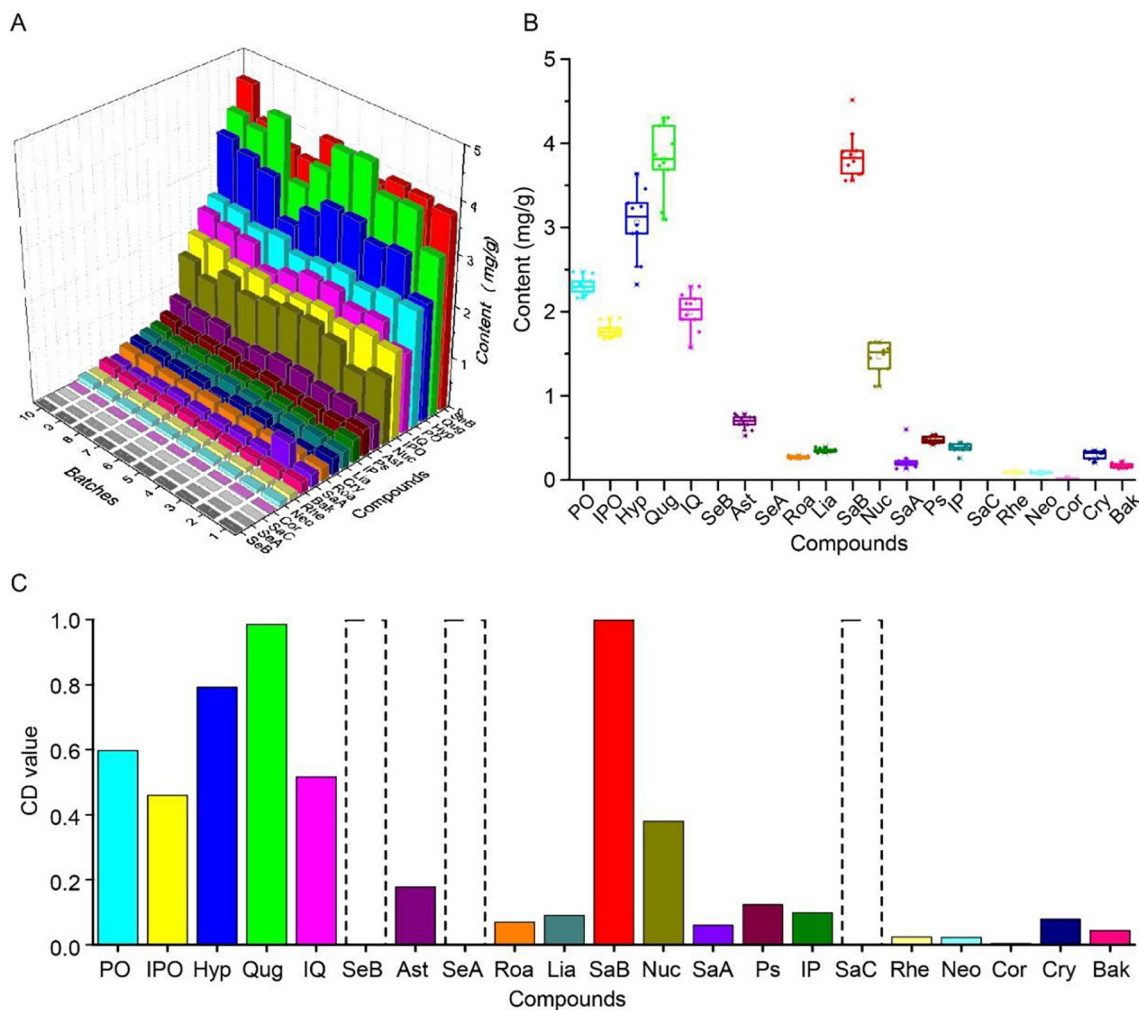
Fig. 2. 3D bar graph (A), box diagram (B) and normalized result (C) for quantitative analysis of 21 candidate compounds in 10 batches of HDTs.

As shown in Fig. 2C, SaB, Qug, Hyp, PO, IQ and IPO displayed the better property in the content dimension with the CD values of 1.000, 0.9853, 0.7921, 0.5975, 0.5161 and 0.4599, respectively, indicating that they can be potentially selected as appropriate Q-Markers from the perspective of content dimension. And Nuc, Ast, Ps, IP, Lia, Cry, Roa, SaA, Bak, Rhe, Neo and Cor were 0.3799, 0.1778, 0.1232, 0.09860, 0.09045, 0.07872, 0.06969, 0.06021, 0.04384, 0.02394, 0.02253 and 0.003867, in sequences.

3.3. Construction of stability dimension of "spider-web" mode upon result of stability for 21 candidate compounds in HDTs

In order to evaluate the property of stability of the tested compounds, HDT samples were stored at high temperature, high humidity and strong light, respectively, and 21 candidate compounds in the collected samples were quantified on 0, 5 and 10 d. As for the changing degree of the focused compounds on content, the content of the candidate compounds on the 10th day divided by that on the 0th day, whose result was further subtracted from 1 according to Eq. (3) as the variation rate (VR). As shown in Fig. 3, the content and the variation rate of 21 candidate compounds in HDTs stored at the different stress conditions were visually displayed, and the detailed data of which were shown in Table S2. Under high humidity and strong light conditions, the content of the tested compounds did not change significantly, except for Neo, Cor, Cry and Bak decreased by 5.05%–28.05%.

However, it was noteworthy that the focused compounds in HDT had poor stability under high temperature condition, which was manifested by the obvious variation rate. The variation rate of PO, IPO, Hyp, Qug, IQ, Ast, Roa, SaB, SaA, Cry and Bak ranged from 21.26% to 34.45%, that of Lia, Neo and Cor was in the range from 10.33% to 14.78%. Nuc, Ps and Rhe were relatively stable with the variation of content below 5%. Besides, the content of IP increased by 8.35%, which may be originated from the conversion from IPO to IP caused by the breakage of glycosidic bond under high temperature condition. SeA, SeB and SaC were also not detected. In general, HDT is sensitive to the conditions of high temperature, high humidity and strong light. The stability index (SI), positively related to stability, was used to objectively describe the stability of the tested compounds. The bigger SI value of the candidate compounds is, the more excellent the stability is. The calculation Eqs. (3) and (4) of VR and SI were as follows:

$$VR_n^m(\%) = (1 - {}^\prime C_n^m / C_n^m) \times 100\% \tag{3}$$

$$SI_n^m = 1 - |VR_n^m| \tag{4}$$

where VR_n^m is the variation rate of the content of the tested compound n in HDT stored at the corresponding stress condition; m is the different stress conditions, including strong light (a), high temperature (b) and high humidity (c); ${}^\prime C_n^m$ is the content of the tested compound n in HDT stored for 10 d under the corresponding stress
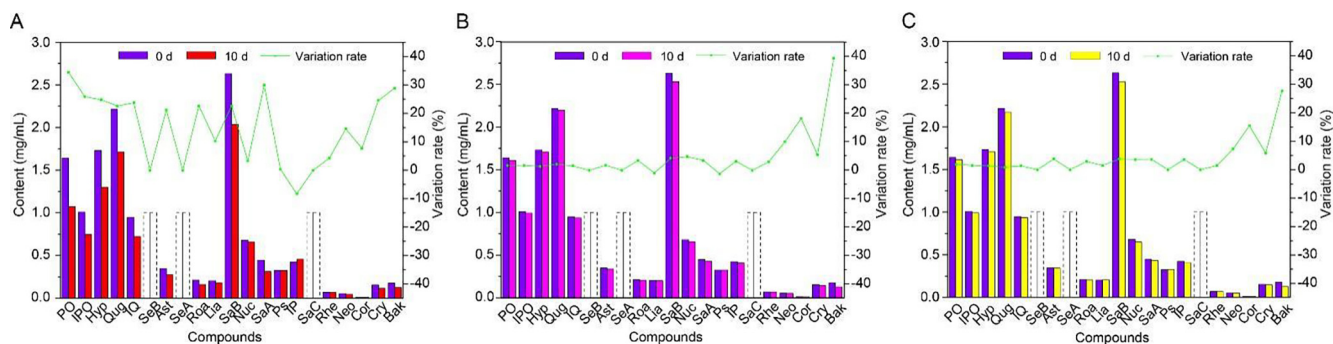
Fig. 3. Double-Y charts for content and change rate of 21 candidate compounds in HDT stored at high temperature (A), high humidity (B) and strong light (C) on 0 and 10 d.

condition; C_n^m is the content of the tested compound n in HDT stored for 0 d under the corresponding stress condition; SI_n^m is the stability index of the tested compound n in HDT stored at the corresponding stress condition.

The SI values of the tested compounds were 0.6555–0.9969, 0.7232–1.000 and 0.7175–0.9902 under the conditions of strong light, high temperature and high humidity, respectively. In order to comprehensively evaluate the stability of the candidate compounds under the different stress conditions, with the help of "spider-web" mode, the general stability index (GSI) of each compound was calculated using the following Eqs. (5) and (6) (Wang et al., 2016). The established "spider-web" mode was shown in Fig. 4A to evaluate the GSI value of each compound. The relative general stability index (R_{GSI}) was employed to normalize the GSI result of tested compounds according to the following Eq. (7). The SI and the R_{GSI} values for 21 candidate compounds in HDT are displayed in Fig. 4B.

$$p_n = \sqrt{\left(SI_n^a\right)^2 + \left(SI_n^b\right)^2} + \sqrt{\left(SI_n^b\right)^2 + \left(SI_n^c\right)^2} + \sqrt{\left(SI_n^c\right)^2 + \left(SI_n^a\right)^2} \quad (5)$$

$$GSI_n = \sqrt{\frac{p_n}{2} \times \sqrt{\frac{p_n}{2} - \sqrt{\left(SI_n^a\right)^2 + \left(SI_n^b\right)^2}}} \\ \times \sqrt{\frac{p_n}{2} - \sqrt{\left(SI_n^b\right)^2 + \left(SI_n^c\right)^2}} \times \sqrt{\frac{p_n}{2} - \sqrt{\left(SI_n^c\right)^2 + \left(SI_n^a\right)^2}} \quad (6)$$

$$R_{GSI(n)} = GSI_n / GSI_{max} \quad (7)$$

where p_n is the perimeter of the triangle connected by points marked with SI_n^a, SI_n^b and SI_n^c in the "spider-web" mode; SI_n^a, SI_n^b and SI_n^c are the stability index of the tested compound n in HDT under strong light (a), high temperature (b) and high humidity (c), respectively. GSI_n is the shaded area of the triangle connected by points marked with SI_n^a, SI_n^b and SI_n^c in the "spider-web" mode; GSI_{max} is the maximum value of GSI among the 21 tested compounds; $R_{GSI(n)}$ is the normalized value for constructing the stability dimension of the tested compound n.

The R_{GSI} value could be employed to build the stability dimension of "spider-web" mode for identifying Q-Markers of HDT. Ps, Rhe, Nuc, Lia and IP showed excellent stability, the R_{GSI} values of which were 1.000, 0.9698, 0.9358, 0.9280 and 0.9115, respectively. And Qug, IQ, Ast, Hyp, IPO, Roa, SaB and Neo had better stability property, the R_{GSI} values of which were 0.8472, 0.8412, 0.8406, 0.8356, 0.8260, 0.8223, 0.8174 and 0.8167, in order. Moreover, the R_{GSI} values of Cry, SaA, PO, Cor and Bak with poor stability were 0.7891, 0.7803, 0.7744, 0.7327 and 0.5212, in turn.

3.4. Evaluation of activity dimension of "spider-web" mode upon antioxidant activity of 21 candidate compounds

For the sake of the rapid and convenient identification of the antioxidant compounds, LC coupled with DPPH· assay has been successfully used in CMM (Li et al., 2012; Shi et al., 2015; Wu et al., 2008). Since the reaction between antioxidants and DPPH· may cause changes in the molecular structure of antioxidants, the peak area of the reacted compounds with antioxidant activity would be obviously reduced or disappeared in the UPLC chromatogram, while compounds without antioxidant activity are almost unchanged. The online UPLC-DPPH· assay method was preformed based on the systematically study of influencing factors, such as reaction concentration and time of reaction between the sample and DPPH·. As shown in Fig. 5, by comparing the UPLC chromatograms of DPPH·-untreated and DPPH·-treated samples, it was obviously found that Hyp (peak 3), Qug (peak 4), IQ (peak 5), Roa (peak 9), Lia (peak 10), SaB (peak 11), unknown compound (peak a) and SaA (peak 13) decreased from 14.06% to 100% according to Eq. (8). Neo (peak 18), as a flavonoid aglycone, was proved to have a weak ability to scavenge radical with DR below 1.74%.

$$DR_n(\%) = (1 - PA_n^t / PA_n^{ut}) \times 100\% \quad (8)$$

where DR_n is the decreased rate of the peak area of the tested compound n in reacted solution; PA_n^t is the peak area of the tested compound n in DPPH·-treated sample; PA_n^{ut} is the peak area of the tested compound n in DPPH·-untreated sample.

In order to verify the above experimental result, the microporous quantitative assay was employed to measure DPPH· scavenging capacity of 18 compounds except for SeA, SeB and SaC, and the IC_{50} value was calculated by plotting the dose–response curve. It can be drawn from Fig. 6A, HDT sample was proved to have better antioxidant activity with the IC_{50} value of 300 μg/mL. From Fig. 6B, SaB was confirmed to have the strongest DPPH· scavenging capacity with IC_{50} value of 5.585 μg/mL in the tested compounds from HDT. Successively, the IC_{50} values of Roa, SaA, IQ, Lia, Hyp, Qug and Neo were 6.319, 6.966, 7.366, 8.366, 8.416, 9.090 and 176.1 μg/mL. The other 10 compounds showed weak antioxidant activity with the SR below 30% at the concentration of above 2 mg/mL. The result was basically consistent with the result of the online UPLC-DPPH· analysis.

The activity index (AI) based on IC_{50} value was used as the evaluation index of the activity dimension of the "spider-web" mode. The Eq. (9) was as follows:

$$AI_n = (1/IC_{50(n)})/(1/IC_{50})_{max} \quad (9)$$

where AI_n is the activity index of antioxidant activity for the tested compound n; $IC_{50(n)}$ is the IC_{50} value of compound n; $(1/IC_{50})_{max}$ is the maximum value of $1/IC_{50}$ among the tested compounds.
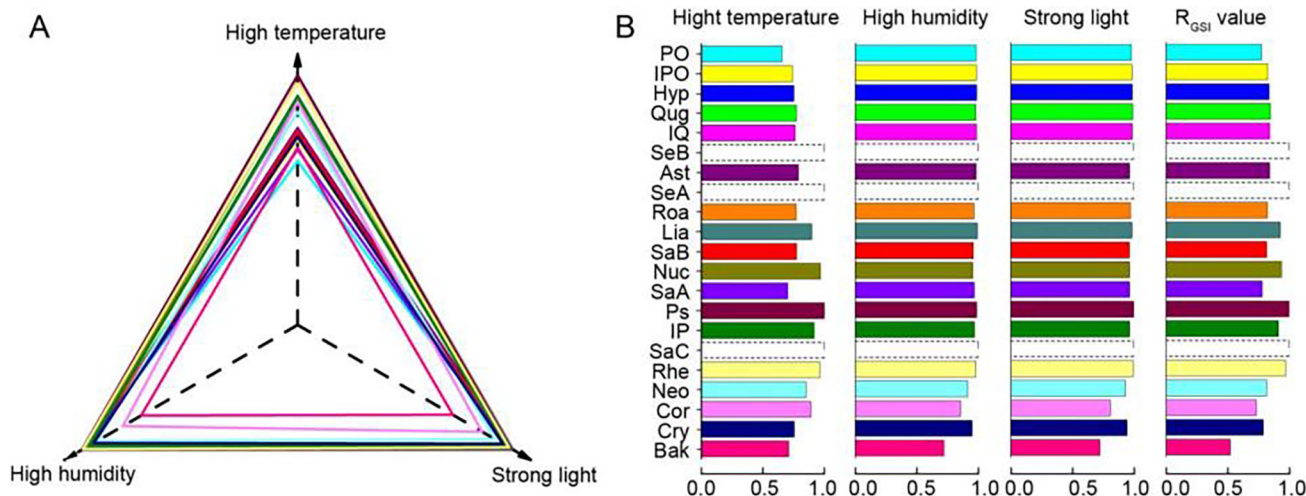
Fig. 4. Established "spider-web" mode for evaluating stability index (A), and result of stability indexes and relative general stability index (B) for 21 candidate compounds.
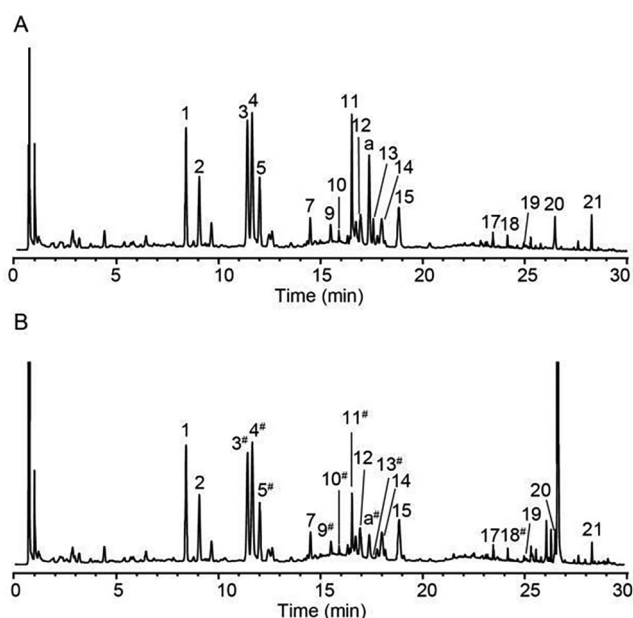

Fig. 5. UPLC chromatograms of DPPH·-untreated sample (A) and DPPH·-treated sample (B) (1. PO, 2. IPO, 3. Hyp, 4. Qug, 5. IQ, 6. SeB, 7. Ast, 8. SeA, 9. Roa, 10. Lia, 11. SaB, 12. Nuc, 13. SaA, 14. Ps, 15. IP, 16. SaC, 17. Rhe, 18. Neo, 19. Cor, 20. Cry, 21. Bak). "#" the compounds with DPPH· scavenging activity proved to be significant decrease of peak area.

From Fig. 6C, the AI values of SaB, Roa, SaA, IQ, Hyp, Lia, Qug and Neo were 1.000, 0.8838, 0.8018, 0.7582, 0.6676, 0.6636, 0.6144 and 0.03171, respectively, which can be possibly selected as suitable Q-Markers from the perspective of activity dimension.

3.5. Regression analysis of "spider-web" mode for identifying Q-Markers of HDT

In view of the result of content, stability and activity dimension, the shaded area of the candidate compounds was constructed by linking points marked with the different dimensions in the "spider-web" mode, which can objectively reflect the contribution of compounds in the complex system of HDT and was regarded as a practical evaluation method for identifying Q-Markers. The larger

the shaded area of the candidate compounds is, the more fitting they are for Q-Markers. Based on the basic principle described in Eqs. (5) and (6), the index of Q-Marker (QMI), the shaded area of the "spider-web" mode, was calculated by general evaluation of "content-stability-activity" of the candidate compounds according to Eqs. (10) and (11).

$$p'_n = \sqrt{(CD_n)^2 + (R_{GSI(n)})^2} + \sqrt{(R_{GSI(n)})^2 + (AI_n)^2} + \sqrt{(CD_n)^2 + (AI_n)^2} \quad (10)$$

$$QMI_n = \sqrt{\frac{p'_n}{2} \times \sqrt{\frac{p'_n}{2} - \sqrt{(CD_n)^2 + (R_{GSI(n)})^2}}} \\ \times \sqrt{\frac{p'_n}{2} - \sqrt{(R_{GSI(n)})^2 + (AI_n)^2}} \\ \times \sqrt{\frac{p'_n}{2} - \sqrt{(CD_n)^2 + (AI_n)^2}} \quad (11)$$

where p'_n is the perimeter of the triangle connected by CD_n, $R_{GSI(n)}$ and AI_n in the "spider-web" mode; QMI_n is the shaded area of the triangle connected by CD_n, $R_{GSI(n)}$ and AI_n in the "spider-web" mode.
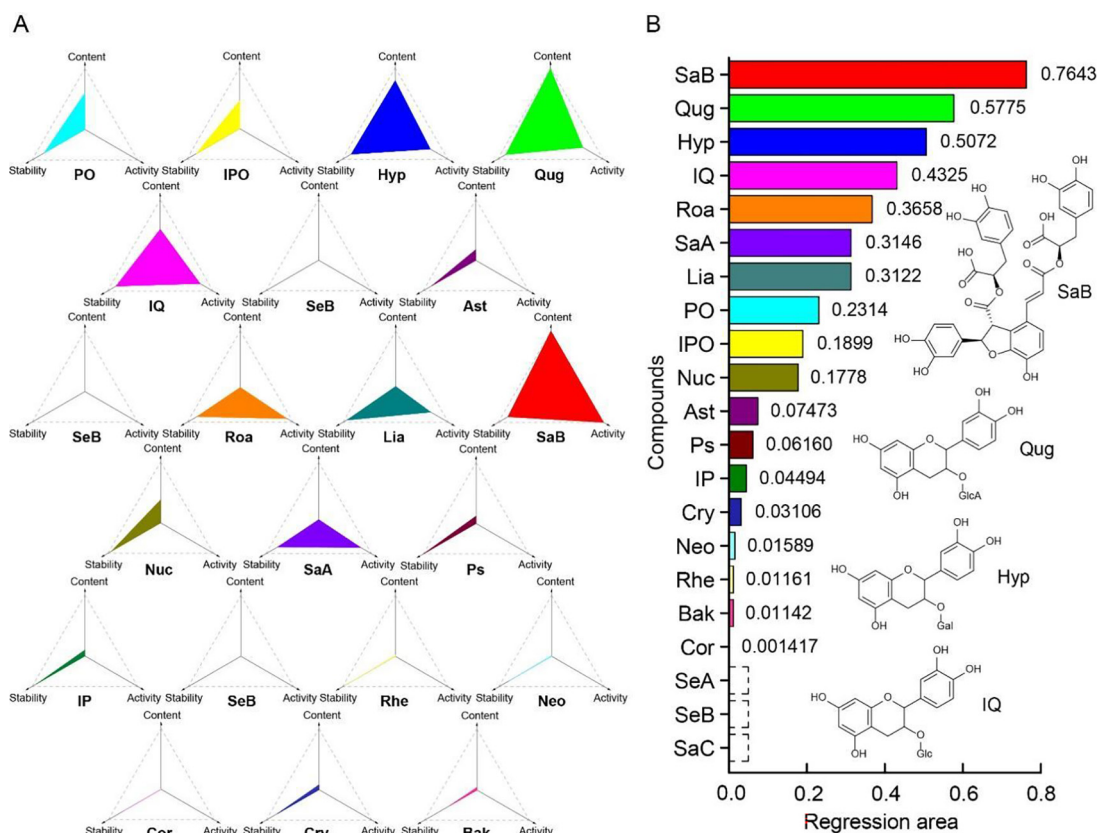
As shown in Fig. 7, the established "spider-web" mode of 21 candidate compounds from HDT and the sequentially identified Q-Markers were visually displayed. In general, the QMIs of candidate compounds except for SeA, SeB and SaC were 0.7643 (SaB), 0.5775 (Qug), 0.5072 (Hyp), 0.4325 (IQ), 0.3658 (Roa), 0.3146 (SaA), 0.3122 (Lia), 0.2314 (PO), 0.1899 (IPO), 0.1778 (Nuc), 0.07473 (Ast), 0.06160 (Ps), 0.04494 (IP), 0.03106 (Cry), 0.01589 (Neo), 0.01161 (Rhe), 0.01142 (Bak) and 0.001417 (Cor), respectively. By taking the actual application into account, SaB, Qug, Hyp and IQ with satisfactory content, stability and activity were served as preferable Q-Markers for HDT.

SaB is a representative compound of phenolic acid in *Salviae Miltiorrhizae Radix* et *Rhizoma*, which is strongly effective in treating many cardiovascular and neurodegenerative diseases (Fan et al., 2018; Li et al., 2020a; Wang et al., 2018; Zhou et al., 2013). Qug, as the active compound from *Nelumbinis Folium*, inhibits lipid peroxidation, ameliorates lipid accumulation in the liver and prevents atherosclerosis (Ohara et al., 2013; Queiroz et al., 2017; Wang et al., 2015). Hyp is one of the major constituents in *Nelumbinis Folium* and *Crataegi Fructus*, which has been proved to have anti-oxidative stress, anti-hyperlipidemia and anti-platelet aggregation effects (Kasimu et al., 2015; Park et al., 2016; Zhang et al., 2017). In addition, IQ is also distributed in *Nelumbinis Folium* and
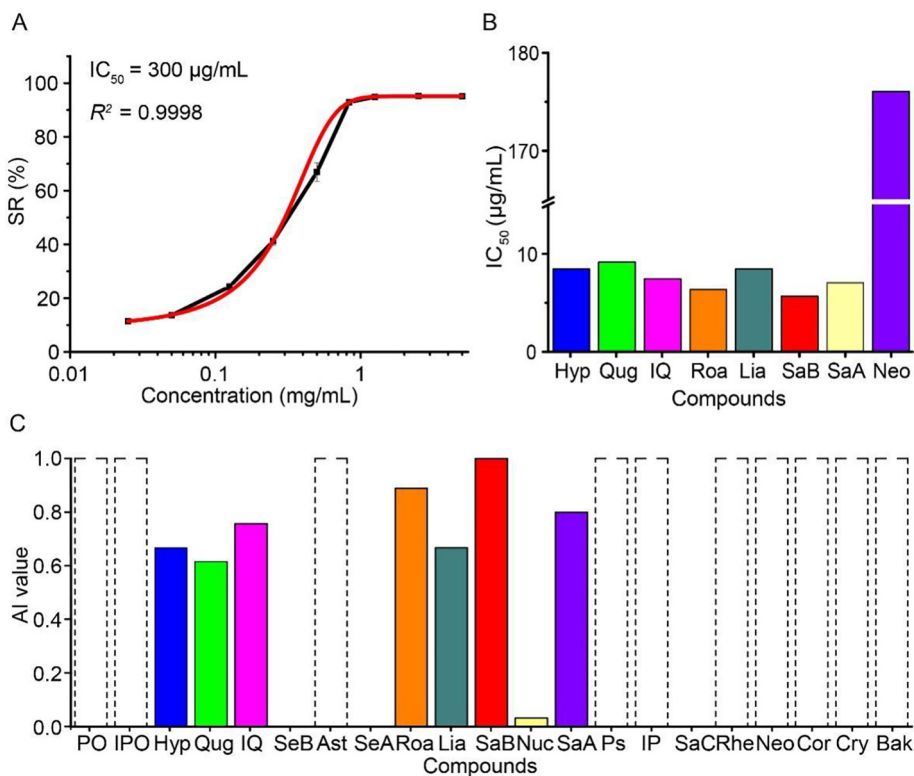
Fig. 6. Dose-effect curve of antioxidant activity of HDT (A), bar chart of IC_{50} values of 21 candidate compounds (B), and normalized result for IC_{50} values of tested compounds (C).

Fig. 7. Established "spider-web" mode of 21 candidate compounds in HDT by taking content, stability and activity into account (A) and the sequentially identified Q-Markers based on the shaded area (B).

Crataegi Fructus, which prevents lipid metabolism disorder and nonalcoholic fatty liver disease (Zhou et al., 2014). And it has been reported to have hypoglycemic, anti-angiogenic, anti-obesity activities, and so on (Lee et al., 2011; Matsubara et al., 2004; Zhang et al., 2018). In a word, SaB, Qug, Hyp and IQ are not only the representative compounds in Chinese herbal medicines of HDT, but also the compounds with superior content, stability and antioxidant activity in HDT. These compounds, as quality control indicators, also have a variety of activities related to hypolipidemia, which are of great significance for evaluating the quality of HDT based on effectiveness and giving full play to its clinical efficacy.

3.6. Identification of Q-Markers related with hepatotoxicity based on our previous researches and literatures

The hepatotoxicity of CMM has attracted much concern, which is directly related to its safety of clinical application. Therefore, it is urgent to identify the Q-Markers related with safety of CMM for quality control and assessment. As the adjuvant in HDT, *Psoraleae Fructus* has the function of tonifying kidney, strengthening *yang*, warming spleen and so on (Xia et al., 2016). In recent years, more and more attention has been paid to hepatotoxicity induced by *Psoraleae Fructus* and its related preparations (Cheung et al., 2009; Duan et al., 2020; Li et al., 2019a). Ps and IP were demonstrated to be culprit, which individually caused liver injury at the dose of 40 and 80 mg/kg for rats by suppression of bile acid excretion in the liver and accumulation of toxin in the hepatocytes (Wang et al., 2019). Another study suggested that chronic exposure at low-level of Ps or IP showed serious and different toxic reaction, resulting in the damage of the visceral organs and the blood system, respectively (Yu et al., 2019). The hepatotoxic mechanism of Ps and IP may be related to a disturbance in amino acids metabolism pathways by serum metabolomics (Yu et al., 2019; Zhang et al., 2019b). As the quality indicator of *Fructus Psoraleae*, the content of original Ps and IP must be 0.70%, which is regulated by the Chinese Pharmacopoeia (Chinese Pharmacopoeia Commission, 2020). Through our study, PO and IPO, the precursor of Ps and IP, were found in *Psoraleae Fructus*, whose content was almost 12 times as high as that of Ps and IP (Yang et al., 2018). Once orally administrated, PO and IPO were metabolized into Ps and IP by gut microbiota, resulting in the accumulation of Ps and IP *in vivo* (Wang et al., 2014). The original and converted Ps and IP would aggravate risk of hepatotoxicity. Therefore, PO, IPO, Ps and IP were strongly recommended as the Q-Markers related with safety for HDT.

4. Conclusion

In this study, the integrated strategy was employed to identify the Q-Markers related to effectiveness and safety for HDT. SaB, Qug, IQ and Hyp were identified as the preferable Q-Markers related with effectiveness by "spider-web" mode based on "content-stability-activity" from the candidate compounds. PO, IPO, Ps and IP were also strongly recommended as Q-Markers closely related with safety by considering hepatotoxicity of the accumulated Ps and IP and conversion between glycoside (PO and IPO) and aglycone (Ps and IP). This study provided scientific evidence for quality control and assessment of HDT, and also provided a meaningful reference for application of Q-Markers in CMM.

Declaration of Competing Interest

The authors declare that they have no known competing financial interests or personal relationships that could have appeared to influence the work reported in this paper.

Appendix A. Supplementary data

Supplementary data to this article can be found online at https://doi.org/10.1016/j.chmed.2021.08.007.

References

Cai, D. (2018). Clinical efficacy oef Hedan tablets combined with fluvastatin and their effects on blood lipid and inflammatory cytokine levels in patients with coronary heart disease. *Journal of Clinical Rational Drug Use, 15*(1), 5–7.

Chen, H., Liu, C., Li, Y., Wu, S., & Chai, Y. (2011). Analysis of the chemical constituents of Hedan Tablet by HPLC-TOF-MS method. *Pharmaceutical Care and Research, 11*(6), 439–443.

Cheung, W. I., Tse, M. L., Ngan, T., Lin, J., Lee, V. K. S., & Poon, W. T. (2009). Liver injury associated with the use of *Fructus Psoraleae* (Bol-gol-zhee or Bu-gu-zhi) and its related proprietary medicine. *Clinical Toxicology, 47*(7), 683–685.

Chinese Pharmacopoeia Commission (2020). *Pharmacopoeia of the People's Republic of China* (Volume I) Beijing: China Medical Science Press.

Davidson, M. H., & Toth, P. P. (2004). Comparative effects of lipid-lowering therapies. *Progress in Cardiovascular Diseases, 47*(2), 73–104.

Duan, J., Dong, W., Xie, L., Fan, S., Xu, Y., & Li, Y. (2020). Integrative proteomics-metabolomics strategy reveals the mechanism of hepatotoxicity induced by *Fructus Psoraleae*. *Journal of Proteomics*, 103767.

Fan, Y., Luo, Q., Wei, J., Lin, R., Lin, L., Li, Y., Chen, Z., Lin, W., & Chen, Q. (2018). Mechanism of salvianic acid B neuroprotection against ischemia/reperfusion induced cerebral injury. *Brain Research, 1679*, 125–133.

Goppel, M., & Franz, G. (2004). Stability control of senna leaves and senna extracts. *Planta Medica, 70*(5), 432–436.

Hajdu, D., Aiglova, K., Vinklerova, I., & Urbanek, K. (2009). Acute cholestatic hepatitis induced by fenofibrate. *Journal of Clinical Pharmacy and Therapeutics, 34*(5), 599–602.

Ho, C. Y., Kuo, T. H., Chen, T. S., Tsay, S. H., Chang, F. Y., & Lee, S. D. (2004). Fenofibrate-induced acute cholestatic hepatitis. *Journal of the Chinese Medical Association, 67*, 245–247.

Hong, X., Tang, H., Wu, L., & Li, L. (2006). Protective effects of the *Alisma orientalis* extract on the experimental nonalcoholic fatty liver disease. *Journal of Pharmacy and Pharmacology, 58*(10), 1391–1398.

Kasimu, R., Fan, Z., Wang, X., Hu, J., Wang, P., & Wang, J. (2015). Anti-platelet aggregation activities of different fractions in leaves of *Apocynum venetum* L. *Journal of Ethnopharmacology, 168*, 116–121.

Lee, S. H., Kim, B., Oh, M. J., Yoon, J., Kim, H. Y., Lee, K. J., & Lee, J. D. (2011). *Persicaria hydropiper* (L.) spach and its flavonoid components, isoquercitrin and isorhamnetin, activate the Wnt/β-catenin pathway and inhibit adipocyte differentiation of 3T3-L1 cells. *Phytotherapy Research, 25*(11), 1629–1635.

Li, A., Gao, M., Zhao, N., Li, P., Zhu, J., & Li, W. (2019a). Acute liver failure associated with *Fructus Psoraleae*: A case report and literature review. *BMC Complementary and Alternative Medicine, 19*(1), 84.

Li, C. L., Liu, B., Wang, Z. Y., Xie, F., Qiao, W., Cheng, J., Kuang, J. Y., Wang, Y., Zhang, M. X., & Liu, D. S. (2020a). Salvianolic acid B improves myocardial function in diabetic cardiomyopathy by suppressing IGFBP3. *Journal of Molecular and Cellular Cardiology, 139*, 98–112.

Li, J. (2012). Effect and safety of Hedan tablet in treatment of hyperlipemia in 39 cases. *Chinese Journal of Integrative Medicine on Cardio-/Cerebrovascuiar Disease, 10*(1), 109–110.

Li, M., Chai, X., Wang, L., Yang, J., & Wang, Y. (2019b). Study of the variation of phenolic acid and flavonoid content from fresh *Artemisiae Argyi Folium* to moxa wool. *Molecules, 24*(24), 4603.

Li, S., Liu, Y., & Chen, X. (2013). Research progress of traditional Chinese medicine in treatment of hyperlipidemia. *Journal of Liaoning University Traditional Chinese Medicine, 15*(6), 138–139.

Li, Y., Chen, Y., Huang, X., Huang, D., Gan, H., Yao, N., Hu, Z., Li, R., Zhan, X., Xie, K., Jiang, J., & Cai, D. (2020b). Tanshinol A ameliorates triton-1339W-induced hyperlipidemia and liver injury in C57BL/6J Mice by regulating mRNA expression of lipemic-oxidative injury genes. *Lipids, 55*(2), 127–140.

Li, Y., Guo, H., Li, A., & Zhang, J. (2016). Rosuvastatin combined with Hedan tablets in treatment of acute cerebral infarction and effect on levels of copeptin and NT-proBNP. *China Journal of Modern Medicine, 26*(22), 59–63.

Li, Y., Wang, X., & Shen, Z. (2017). Traditional Chinese medicine for lipid metabolism disorders. *American Journal of Translational Research, 9*(5), 2038–2049.

Li, Y. J., Chen, J., Li, Y., & Li, P. (2012). Identification and quantification of free radical scavengers in the flower buds of *Lonicera* species by online HPLC-DPPH assay coupled with electrospray ionization quadrupole time-of-flight tandem mass spectrometry. *Biomedical Chromatography, 26*(4), 449–457.

Liao, J., Tian, J., Li, T., Song, W., Zhao, W., & Du, J. (2014). Xuefuzhuyu decoction for hyperlipidemia: A systematic review and meta-analysis of randomized clinical trails. *Journal of Traditional Chinese Medicine, 34*(4), 411–418.

Liu, C. (2021). Five-year review on development of quality markers of traditional Chinese medicine. *Chinese Traditional and Herbal Drugs, 52*(9), 2511–2518.

Liu, C., Chai, Y., Zhu, Z., & Liu, F. (2011). High performance liquid chromatography determination of nuciferine tanshinone psoralen and isopsoralen in compound hedan pills. *Pharmaceutical Journal of Chinese People's Liberation Army, 27*(1), 57–60.

Liu, C., Chen, S., Xiao, X., Zhang, T., Hou, W., & Liao, M. (2016). A new concept on quality marker of Chinese materia medica: Quality control for Chinese medicinal products. *Chinese Traditional and Herbal Drugs, 47*(9), 1443–1457.

Liu, C., Cheng, Y., Guo, D. A., Zhang, T., Li, Y., Hou, W., Huang, L., & Xu, H. (2017). A new concept on quality marker for quality assessment and process control of Chinese medicines. *Chinese Herbal Medicines, 9*(1), 3–13.

Liu, F., Lin, H., Wu, D., Wang, Z., Xu, D., Xiao, F., Chen, D., & Wang, S. (2015). Study on dissolution and degradation characteristics of phenolic acids in water extract of Danshen decoction. *Journal of Guangzhou University of Traditional Chinese Medicine, 32*(3), 489–493.

Matsubara, K., Ishihara, K., Mizushina, Y., Mori, M., & Nakajima, N. (2004). Anti-angiogenic activity of quercetin and its derivatives. *Letters in Drug Design & Discovery, 1*, 329–333.

Navar-Boggan, A. M., Peterson, E. D., D'Agostino, R. B., Sr., Neely, B., Sniderman, A. D., & Pencina, M. J. (2015). Hyperlipidemia in early adulthood increases long-term risk of coronary heart disease. *Circulation, 131*(5), 451–458.

Ohara, K., Wakabayashi, H., Taniguchi, Y., Shindo, K., Yajima, H., & Yoshida, A. (2013). Quercetin-3-O-glucuronide induces ABCA1 expression by LXRα activation in murine macrophages. *Biochemical and Biophysical Research Communications, 441*(4), 929–934.

Park, J. Y., Han, X., Piao, M. J., Oh, M. C., Fernando, P. M., Kang, K. A., Ryu, Y. S., Jung, U., Kim, I. G., & Hyun, J. W. (2016). Hyperoside induces endogenous antioxidant system to alleviate oxidative stress. *Asian Pacific Journal of Cancer Prevention, 21* (1), 41–47.

Pencina, M. J., Navar-Boggan, A. M., D'Agostino, R. B., Sr, Williams, K., Neely, B., Sniderman, A. D., et al. (2014). Application of new cholesterol guidelines to a population-based sample. *The New England Journal of Medicine, 60*(2), 534.

Queiroz, M., Oppolzer, D., Gouvinhas, I., Silva, A. M., Barros, A., & Dominguez-Perles, R. (2017). New grape stems' isolated phenolic compounds modulate reactive oxygen species, glutathione, and lipid peroxidation *in vitro*: Combined formulations with vitamins C and E. *Fitoterapia, 120*, 146–157.

Sham, T. T., Chan, C. O., Wang, Y. H., Yang, J. M., Mok, D. K., & Chan, S. W. (2014). A review on the traditional Chinese medicinal herbs and formulae with hypolipidemic effect. *Biomed Research International, 2014*, 925302.

Shi, Q., Chen, J., Zhou, Q., Lei, H., Luan, L., Liu, X., et al. (2015). Indirect identification of antioxidants in Polygalae Radix through their reaction with 2,2-diphenyl-1-picrylhydrazyl and subsequent HPLC-ESI-Q-TOF-MS/MS. *Talanta, 144*, 830–835.

Sun, L., Xu, F., Ge, Z., Shen, X., & An, D. (2017). The effect of Hedan Decoction on the expression of interleukin-1β and tumor necrosis factor-α of atherosclerotic in ApoE (-/-) mice. *Journal of Emergency in Traditional Chinese Medicine, 26*(7), 1137–1140.

Tian, M. (2010). Study on therapeutic effect of dimethylbiguanide combined with Hedan Tablet in the treatment of non-alcoholic steatohepatitis. *Chinese General Practice, 13*(33), 3811–3812.

Tian, W., Lan, S., Zhang, L., Sun, L., Huang, J., Yang, X., et al. (2017). Safety evaluation and risk control measures of *Psoralea corylifolia*. *China Journal of Chinese Materia Medica, 42*(21), 4059–4066.

Wang, C., Luo, H., Xu, Y., Tao, L., Chang, C., & Shen, X. (2018). Salvianolic acid B-alleviated angiotensin II induces cardiac fibrosis by suppressing NF-κB pathway *in vitro*. *Medical Science Monitor, 24*, 7654–7664.

Wang, L., Zhang, Z., Wu, S., & Shang, J. (2015). Effect of quercetin-3-O-β-D-glucuronide on free fatty acid induced steatosis in HepG2 cells. *Journal of China Pharmaceutical University, 46*(5), 587–593.

Wang, Q. (2015). Clinical observation of Hedan Tablets combined with rosuvastatin in treatment of type 2 diabetes with hyperlipidemia. *Drugs & Clinic, 30*(6), 670–673.

Wang, Y., Jiang, Z., Yang, F., Chai, X., Zhu, Y., Zhao, X., et al. (2016). Establishment of a ternary network system for evaluating the antioxidant fraction of Danhong injection. *Biomedical Chromatography, 30*(10), 1666–1675.

Wang, Y., Zhang, H., Jiang, J. M., Zheng, D., Chen, Y. Y., Wan, S. J., Tan, H. S., Tang, L. M., & Xu, H. X. (2019). Hepatotoxicity induced by psoralen and isopsoralen from *Fructus Psoraleae*: Wistar rats are more vulnerable than ICR mice. *Food and Chemical Toxicology, 125*, 133–140.

Wang, Y. F., Liu, Y. N., Xiong, W., Yan, D. M., Zhu, Y., Gao, X. M., Xu, Y. T., & Qi, A. D. (2014). A UPLC-MS/MS method for *in vivo* and *in vitro* pharmacokinetic studies of psoralenoside, isopsoralenoside, psoralen and isopsoralen from *Psoralea corylifolia* extract. *Journal of Ethnopharmacology, 151*(1), 609–617.

Wierzbicki, A. S., Hardman, T. C., & Viljoen, A. (2012). New lipid-lowering drugs: An update. *International Journal of Clinical Practice, 66*(3), 270–280.

Wu, J. H., Huang, C. Y., Tung, Y. T., & Chang, S. T. (2008). Online RP-HPLC-DPPH screening method for detection of radical-scavenging phytochemicals from flowers of *Acacia confusa*. *Journal of Agricultural and Food Chemistry, 56*(2), 328–332.

Wu, Y. J., Hong, C. Y., Lin, S. J., Wu, P., & Shiao, M. S. (1998). Increase of vitamin E content in LDL and reduction of atherosclerosis in cholesterol-fed rabbits by a water-soluble antioxidant-rich fraction of *Salvia miltiorrhiza*. *Arteriosclerosis, Thrombosis, and Vascular Biology, 18*(3), 481–486.

Xia, W., Sun, C., Zhao, Y., & Wu, L. (2011). Hypolipidemic and antioxidant activities of sanchi (*Radix Notoginseng*) in rats fed with a high fat diet. *Phytomedicine, 18* (6), 516–520.

Xia, Y., Yu, L., Wang, D., Cui, Y., Xiong, R., & Zhang, M. (2016). Study on the effects of different processed products of *Fructus Psoralea* on kidney yang deficiency, spleen deficiency rats. *Asia-Pacific Traditional Medicine, 12*(9), 5–7.

Xu, R. X., Wu, N. Q., Li, S., Zhang, Y., Li, X. L., Guo, Y. L., et al. (2016). Effects of Hedan Tablet on lipid profile, proprotein convertase subtilisin/kexin type 9 and high-density lipoprotein subfractions in patients with hyperlipidemia: A primary study. *Chinese Journal of Integrative Medicine, 22*(9), 660–665.

Yang, J., Yang, J., Du, J., Feng, Y., Chai, X., Xiao, M., et al. (2018). General survey of *Fructus Psoraleae* from the different origins and chemical identification of the roasted from raw *Fructus Psoraleae*. *Journal of Food and Drug Analysis, 26*(2), 807–814.

Yu, H., Yang, J., Ding, J., He, Y., Jiang, Z., Chai, X., et al. (2018). Stability study and identification of degradation products of caffeoylgluconic acid derivatives from *Fructus Euodiae*. *Molecules, 23*(8), 1975.

Yu, Y., Wang, P., Yu, R., Lu, J., Jiang, M., & Zhou, K. (2019). Long-term exposure of psoralen and isopsoralen induced hepatotoxicity and serum metabolites profiles changes in female rats. *Metabolites, 9*(11), 263.

Zhang, J., Wang, D., Zhang, X., Yang, J., Chai, X., & Wang, Y. (2020). Application of "spider-web" mode in discovery and identification of Q-markers from Xuefu Zhuyu capsule. *Phytomedicine, 77*, 153273.

Zhang, J., Yang, J., Chai, X., Wang, Y., & Yang, J. (2019a). The study of powder homogenization for *Fructus Psoraleae*. *Tianjin Journal of Traditional Chinese Medicine, 36*(7), 710–714.

Zhang, L., Zhang, S. T., Yin, Y. C., Xing, S., Li, W. N., & Fu, X. Q. (2018). Hypoglycemic effect and mechanism of isoquercitrin as an inhibitor of dipeptidyl peptidase-4 in type 2 diabetic mice. *RSC Advances, 8*, 14967–14974.

Zhang, Y., Yang, L., Bi, Y., Yuan, X., Shi, H., & Zhou, K. (2019b). Seven-day intragastric administration of isopsoralen-induced hepatotoxicity and serum metabonomics in rats. *Journal of Toxicology, 33*(4), 289–293.

Zhang, Z., Zhang, D., Du, B., & Chen, Z. (2017). Hyperoside inhibits the effects induced by oxidized low-density lipoprotein in vascular smooth muscle cells via oxLDL-LOX-1-ERK pathway. *Molecular and Cellular Biochemistry, 433*(1–2), 169–176.

Zhang, Z., Zhou, G., & Cheng, W. (2015). Effects of Hedan Tablet on hypersensitive C-reactive protein in patients with dyslipidemia. *Chinese Journal of Integrative Medicine on Cardio-/Cerebrovascuiar Disease, 13*(17), 1988–1989.

Zhao, L., & Tang, S. (2013). Simultaneous determination of eight components in Hedan Tablets by UPLC. *Chinese Traditional and Herbal Drugs, 44*(16), 2257–2260.

Zhao, S. P., Liu, L., Cheng, Y. C., & Li, Y. L. (2003). Effect of Xuezhikang, a cholestin extract, on reflecting postprandial triglyceridemia after a high-fat meal in patients with coronary heart disease. *Atherosclerosis, 168*(2), 375–380.

Zhou, C., Liu, J., Gao, H., Lai, X., & Qiu, S. (2013). Hypotensive effect of salvianolic acid B on spontaneous hypertensive rats. *Traditional Chinese Drug Research and Clinical Pharmacology, 24*(4), 374–379.

Zhou, J., Yoshitomi, H., Liu, T., Zhou, B., Sun, W., Qin, L., Guo, X., Huang, L., Wu, L., & Gao, M. (2014). Isoquercitrin activates the AMP-activated protein kinase (AMPK) signal pathway in rat H4IIE cells. *BMC Complementary and Alternative Medicine, 14*, 42.